Caught in the cosmic web: environmental effects on subhalo abundance and internal density profiles

Journal Club

SWIFAR, 2024/09/18

Background

The cosmic web originates from the gravitational amplification of the small Gaussian density fluctuations present within the primordial plasma.

Four components:

1. High-density nodes - inhabited primarily by galaxy clusters, groups and extremely massive galaxies;
2. Filament;
3. Walls- flattened walls spanning the nearly empty space between the filaments;
4. Voids

Matter evacuated from voids

Structure Emerge

Background

1. This anisotropic **gravitational collapse** driving the emergence of the cosmic web is also **responsible for** the **hierarchical assembly of dark matter halos** on smaller scales;

2. Baryons accumulate deep within the potential wells of DM halos;

The properties of galaxies are sensitive to their host halos and environments.

Attempts to connect DM halo properties with the cosmic web

Gao et al. 2005; Wang et al. 2007,

1) Most massive DM halos are found only in the highest density cosmic web environments;

2) Their abundance, concentrations, and assembly histories are similarly correlated with environmental density.

Aragón-Calvo et al. 2007b; Hahn et al. 2007a,b; Libeskind et al. 2012; Forero-Romero et al. 2014; Ganeshaiah Veena et al. 2018, 2019, 2021

Halo spins and shape align with the principal axes of the filaments, or aligned towards the centers of the nearest void.

Aragon Calvo et al. 2019; Malavasi et al. 2022, Xu et al. 2020

Hydrodynamic simulations show that galaxy properties such as star formation rates and angular momentum exhibit a similar dependence on the large-scale environment.

Wang et al. 2017, Zhang et al. 2021, Dressler 1980, Miraghaei 2020

Observational studies of galaxies have also shown that their mass and luminosity, formation times, morphological properties, as well as the activity of the active galactic nucleus, are influenced by the nature of their environment.

Motivation

The abundance and the internal properties of subhalos;

Previous: previous studies have examined how these properties depend on their host.

This work: expands these analyses to consider the influence of the cosmic web environments surrounding their hosts.

Goal: is to address this gap in understanding and, using gravity-only numerical simulations, to connect the present-day properties of subhalo populations with the cosmic web environments of their hosts.

Methodology

利用引力势的 Hessian 矩 阵来描述暗晕周围大尺度环境

这里潮汐场 T_{ij} 由引力势的 Hessian 矩阵给出：

$$T_{ij} = \partial_{ij}\phi$$

因此靠近语句引力势极值附近的运动可以完全由潮汐场的本征值核本征方向确定: $\lambda_1 > \lambda_2 > \lambda_3$

空洞： 均为负；

Wall: $\lambda_1 > 0, \lambda_{2,3} < 0$；

Filament: $\lambda_1 > \lambda_2 > 0, \lambda_3 < 0$；

Node: $\lambda_1 > \lambda_2 > \lambda_3 > 0$

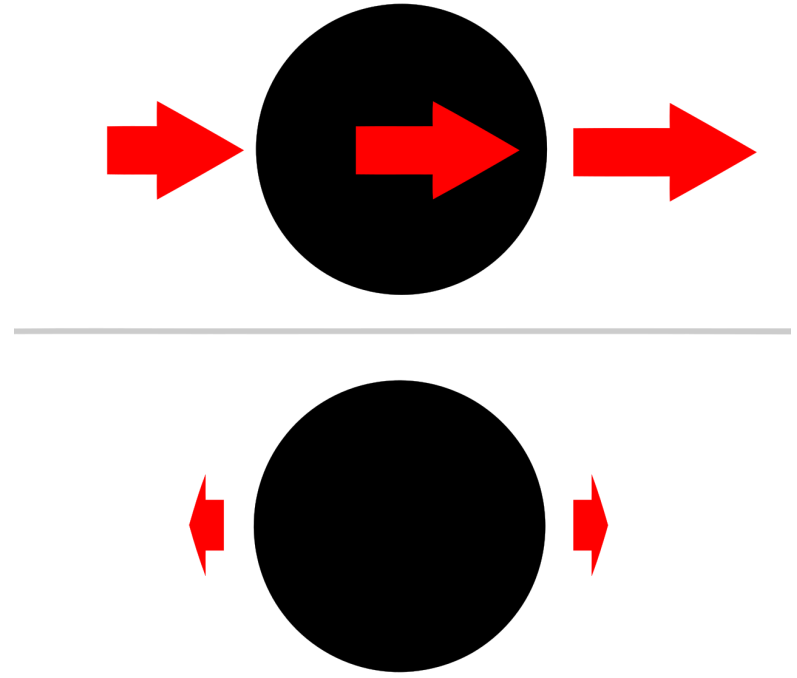

Methodology-Cosmic web segmentation

1. First, we smooth the DM **density field**, with a Gaussian filter and adopt several smoothing scales, R_n, resulting in a smoothed field, $f_{\mathrm{R}_n}(\vec{x})$.

$$f(\vec{x}) \equiv \frac{\rho(\vec{x})}{\langle\rho\rangle},$$

2. Second, for each filtering scale the Hessian matrix is calculated via:

$$\mathrm{H}_{ij,R_n}(\vec{x}) = R_n^2 \left(\partial^2 f_{R_n(\vec{x})} / \partial x_i \partial x_j\right)$$

3. Hessian eigenvalue for different environments

Structure	Soft constraints	Strict constraints
Cluster	$\lvert\lambda_1\rvert \simeq \lvert\lambda_2\rvert \simeq \lvert\lambda_3\rvert$	$\lambda_1 < 0; \lambda_2 < 0; \lambda_3 < 0$
Filament	$\lvert\lambda_1\rvert \simeq \lvert\lambda_2\rvert \gg \lvert\lambda_3\rvert$	$\lambda_1 < 0; \lambda_2 < 0$
Wall	$\lvert\lambda_1\rvert \gg \lvert\lambda_2\rvert; \lvert\lambda_1\rvert \gg \lvert\lambda_3\rvert$	$\lambda_1 < 0$

4. Repeat step1-3 for each smoothing scale, and the resulting environmental signatures are combined into ***one parameter***-free, multi-scale signature, $S(x) = \max[S_{R_n}(x)]$

5. Assign cosmic web environments:

Clusters: The regions satisfying all of the following criteria are classified as clusters:

Cluster environment

- The cluster signature, $S_c > S_c^{\text{thresh}}$.
- The mass is greater than $5 \times 10^{14}\ h^{-1}\,\mathrm{M}_\odot$.
- The mean density is greater than $300\rho_c(z)$.

The shape strength

$$\mathcal{I} = \begin{cases} \left|\frac{\lambda_3}{\lambda_1}\right| & \text{cluster,} \\ \left|\frac{\lambda_2}{\lambda_1}\right| \Theta\left(1 - \left|\frac{\lambda_3}{\lambda_1}\right|\right) & \text{filament,} \\ \Theta\left(1 - \left|\frac{\lambda_2}{\lambda_1}\right|\right) \Theta\left(1 - \left|\frac{\lambda_3}{\lambda_1}\right|\right) & \text{wall,} \end{cases} \tag{6}$$

where we use the notation $\Theta(x) = x\theta(x)$ for clarity, with $\theta(x)$ the step function ($\theta(x) = 1$ if $x \geq 0$, 0 otherwise). The strength $\mathcal{I}$ is large when the eigenvalues at $\boldsymbol{x}$ correspond to a prominent structure and small otherwise. The cluster/filament/wall signature is defined as

$$\mathcal{S} = \mathcal{I} \times \begin{cases} |\lambda_3|\ \theta(-\lambda_1)\theta(-\lambda_2)\theta(-\lambda_3) & \text{cluster,} \\ |\lambda_2|\ \theta(-\lambda_1)\theta(-\lambda_2) & \text{filament,} \\ |\lambda_1|\ \theta(-\lambda_1) & \text{wall,} \end{cases} \tag{7}$$

Cautun,2013

Filaments/Wall: $S_{\mathrm{f}}^{\mathrm{thresh}} \equiv \max \left| \frac{\partial M(S_{\mathrm{f}})^2}{\partial S_{\mathrm{f}}} \right|$.

$M_f(s_f)$ ∴ the mass in filaments with a signature value larger or equal to S_f.

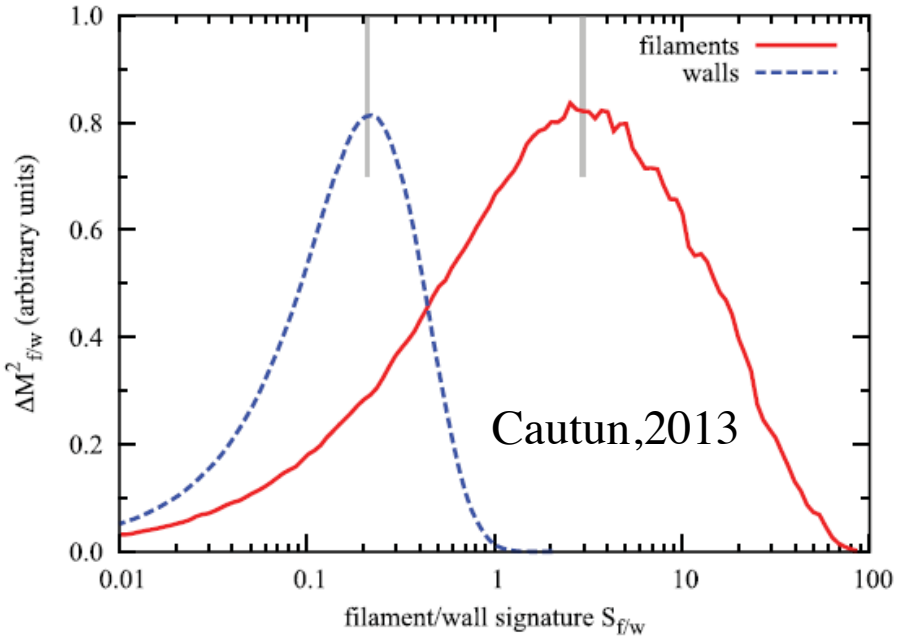

Figure 3. Upper panel: the dependence of the fraction of clusters with density larger than the virial density versus the cluster signature $\mathcal{S}_c$. The intersection of the grey lines shows the cluster detection threshold. Lower panel: determination of the detection threshold for filaments and walls. The peak of ΔM^2 (shown by the grey vertical lines) corresponds to the signature threshold for filament and wall identification (see text for details).

Simulations

the COpernicus complexio LOw Resolution (COLOR) simulation

Np	m_p	L	Cosmology
1620^3	$6.19\times10^9 M_\odot/h$	$70.4Mpc/h$	WMAP-7

DM halos: FoF with b=0.2 , use M_{200} as the host halo mass

Halos in Filament/wall/void

In this analysis, we ignore the 'node' environment and focus only on the host halo samples in **filaments**, **walls**, and **voids**. Because they facilitate the creation of samples of **unperturbed** host halos in each environment

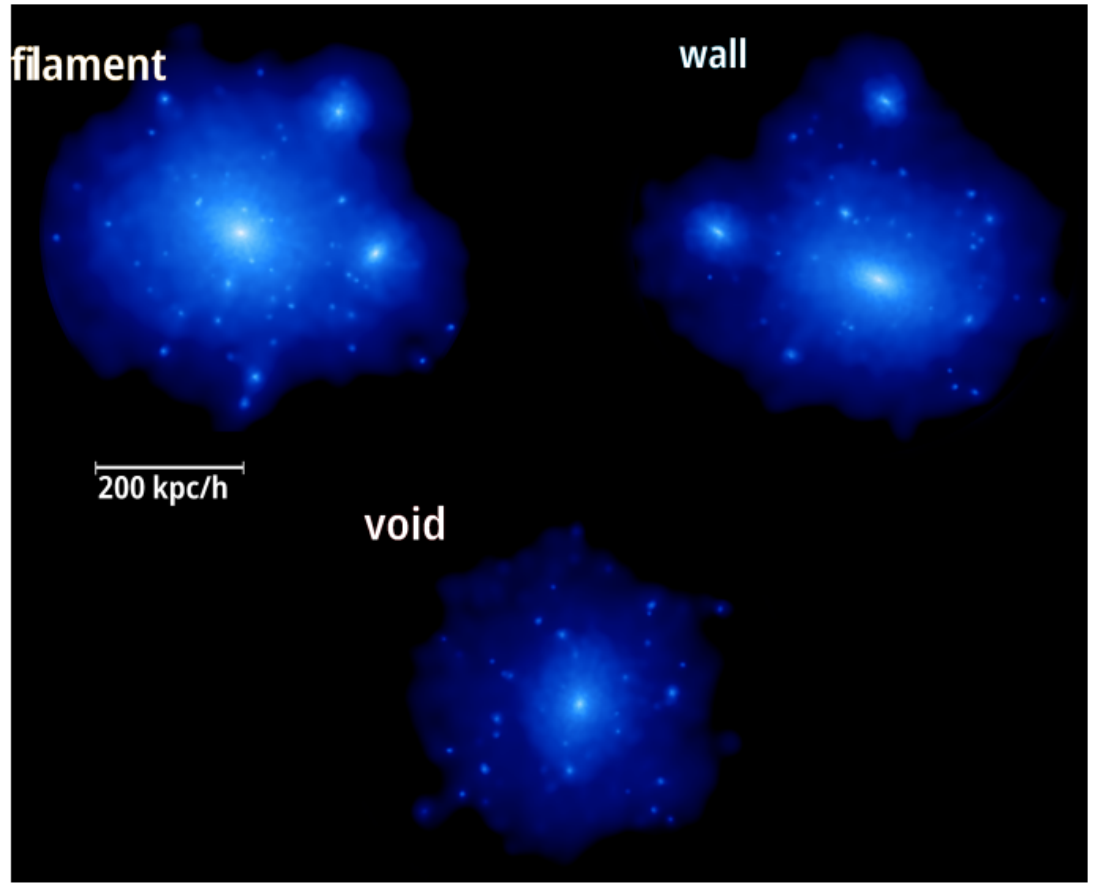

Fig. 1. Renderings of the projected density of DM in three similarly massive halos selected from different cosmic web environments identified by CaCTus. Moving clockwise from the upper-left, the halos are selected from a filament, wall, and void environment, and have masses of $M_{200} = 8.3 \times 10^{11}$, 7.0×10^{11}, and $3.5 \times 10^{11}\ h^{-1}\,\mathrm{M}_{\odot}$, respectively. The void halo presented here is one of the most massive found in that environment in the COLOR volume. After adjusting for the factor of two in halo mass, the most striking difference is the relative lack of massive subhalos in the void host when compared to the other two.

The dependence of subhalo population properties on the cosmic web

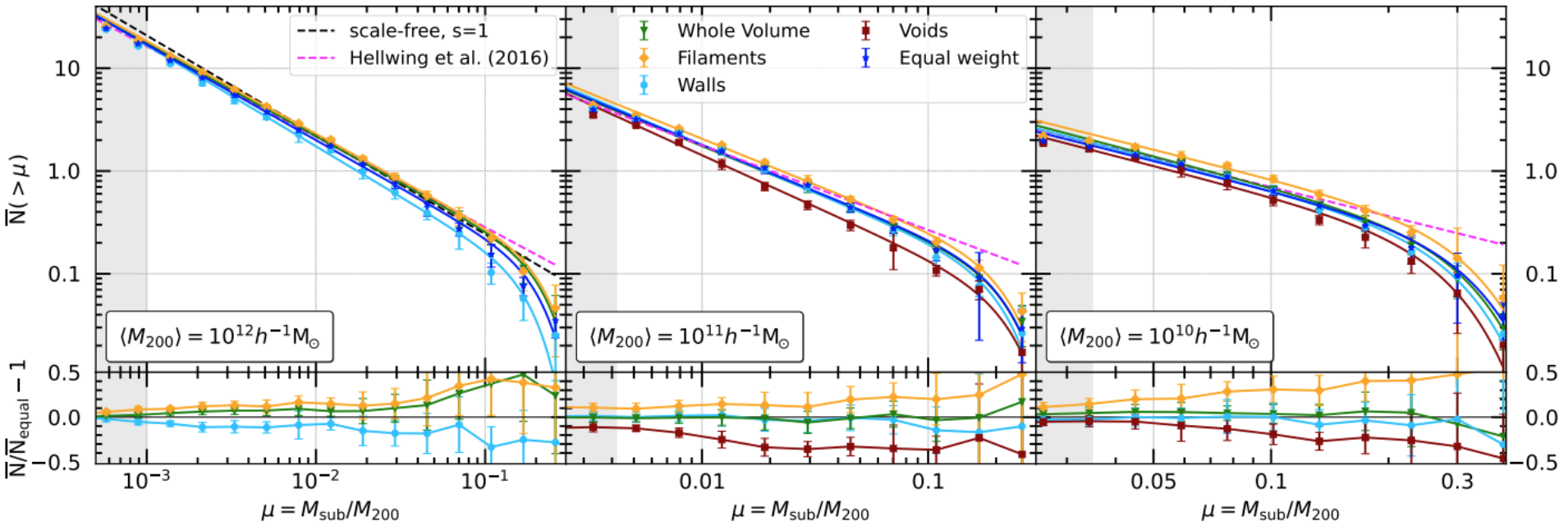

Fig. 2. *Upper panels:* The median cumulative subhalo mass functions corresponding to host halos in three different mass bins, $\langle M_{200}\rangle$, shown as data points, sampled from different environments: whole volume (green triangles), filaments (yellow diamonds), walls (light blue circles), voids (dark-red squares), and our synthetic equally weighted sample (dark blue stars). The error bars show bootstrapped 68% errors on the medians. The solid lines with matching colours indicate the best-fits to the exponential power-law model from Eq. (4). The gray shaded regions at the left of each panel indicate the subhalo resolution limit, μ_{min}. Finally, the two dashed lines illustrate the single power-law models for the scale-free case (black) and the best-fit from the COCO simulations (magenta) of Hellwing et al. (2016). *Lower panels:* The ratio of each subhalo mass function taken with respect to the equally weighted sample. Note the different ranges of the x-axes among the panels.

the fraction of the total mass of halos contained in subhalos

$$f_{\rm sub}(\geq \mu_0) = \int_{\mu_0}^{1} \mu \frac{{\rm d}N}{{\rm d}\mu} \, .$$

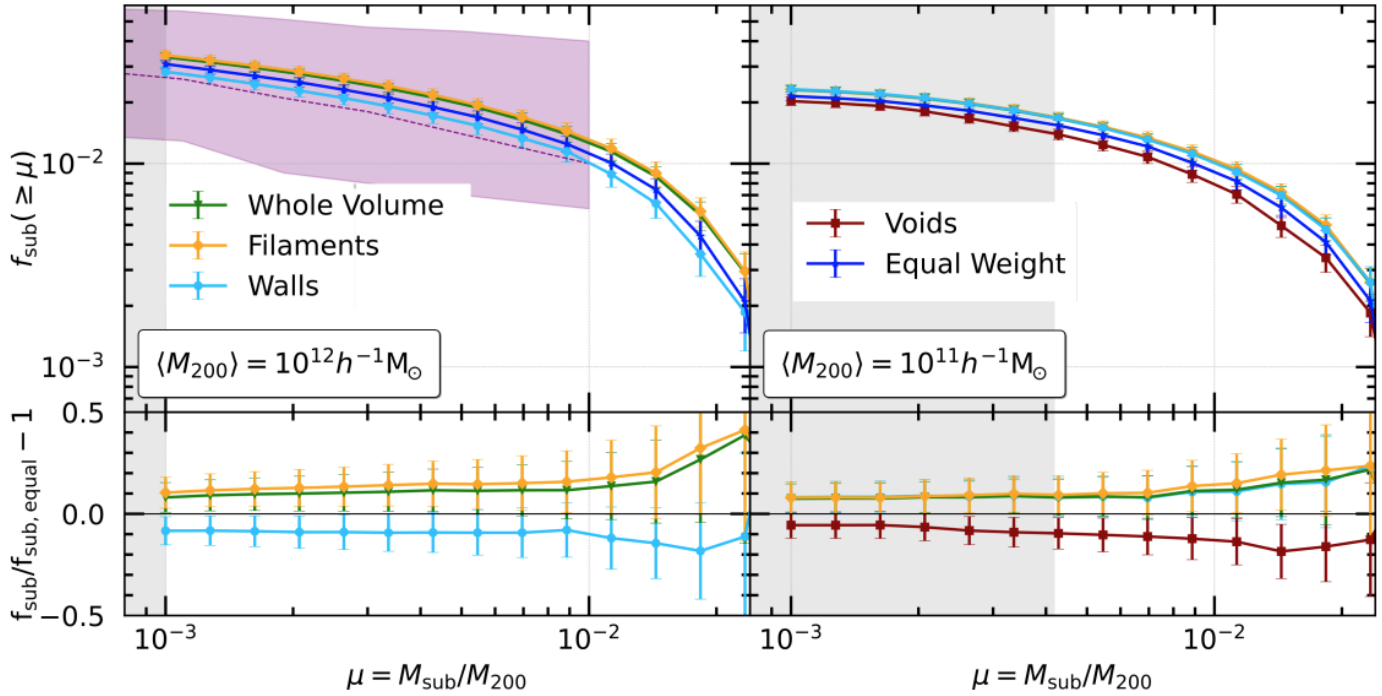

Fig. 3. *Upper panels:* The fraction of the host halo mass in substructures. We show the same environmental samples as in Fig. 2 for the two mass bins where the μ ranges are above the resolution limits. As before, the error bars correspond to the bootstrapped 68% errors on the medians. The gray shaded regions at the left of each panel show the subhalo resolution limit of the simulation. *Lower panels:* The ratios of the substructure mass fraction in each environment with respect to the equally weighted sample. The error bars correspond to the bootstrap error on the median. For comparison, we show the median and 60% scatter (dashed line and shaded region) from the MILLENNIUM II simulation (Gao et al. 2011).

- At fixed host mass, the abundance of subhalos depends on the cosmic web environment of their hosts (Fig. 2). Host halos with $\langle M_{200} \rangle = 10^{10}\ h^{-1}\,\mathrm{M}_{\odot}$ in filaments have as much as three times more massive subhalos than hosts with the same mass in voids. At subhalo masses below $0.1M_{200}$, the abundance of subhalos in filament halos is only 50% greater than in void halos. The size of these differences decreases as the host halo mass is increased.
- The measure of the halo *granularity*, the mass fraction in subhalos, f_{sub}, shows a sizeable and significant variation with the cosmic web (Fig. 3). Here, typically filament hosts tend to be more granular, while void halos are characterized by a smoother density distribution. Generally, lower mass hosts show stronger dependence on the cosmic web.
- The absolute difference in velocity functions between different environments is smaller than the difference in mass functions (Fig. 4). This is because subhalos with similar masses can have very different V_{max}.
- The relative differences between the velocity functions in various environments are generally smaller than what we observe for mass functions. Generally, we start to observe greater than 10% environmental difference in the velocity function above $0.5V_{200}$ for the most massive host bin. For lower-mass hosts the differences are seen for a larger range of subhalo v values.
- Subhalos in filaments are most concentrated, and those in voids are least concentrated (Fig. 5). This is approximately a 10% effect across all host mass bins, although in the $10^{12}\ h^{-1}\,\mathrm{M}_{\odot}$ bin it is largely absent below $V_{\mathrm{max}} = 80\ \mathrm{km\,s^{-1}}$.
- The characteristic density profile also displays a dependence on the parent halo mass by showing a reduction of R_{max} value as the host halo mass decreases.

summary

In this paper, we have analyzed the impact of the cosmic web environment on the subhalo populations of host halos at $z = 0$.